中国激光

银微纳颗粒复合薄膜连接接头高保温组织性能演变

王文淦，贾强，阿占文，冯斌，赵文正，白海林，邹贵生*

清华大学机械工程系摩擦学国家重点实验室，北京 100084

摘要 采用脉冲激光沉积方法在待连接母材表面沉积制备无有机物的银微纳颗粒复合薄膜，用该薄膜作为中间层低温烧结连接 SiC 芯片与金属化陶瓷基板。将连接接头置于大气、真空及氧气含量可控环境进行 300 ℃高温存储实验，系统研究了保温环境对接头多孔连接层的组织演变和性能影响规律。结果表明：保温 2000 h 以内，接头在室温下的剪切强度均高于 20 MPa 且明显高于美国军标。大气环境保温 0～400 h 期间，连接层内部孔隙逐渐聚集并导致组织致密化，接头强度提升；保温 400～2000 h 期间的孔隙聚集与扩大导致孔隙率明显增加，强度逐渐下降。真空环境对连接层内孔隙演变存在阻碍作用。保温环境的氧浓度提升可加速烧结连接层组织在高温存储过程中的演变进程。

关键词 激光技术；材料；银微纳颗粒复合薄膜；脉冲激光沉积；低温烧结连接；高温可靠性

中图分类号 O436 **文献标志码** A **doi**：10.3788/CJL202148.0802015

1 引言

随着新一代功率电子器件逐步投入市场化应用，其应对严苛工况条件的优势也逐步显现。其中，以 SiC 功率芯片为代表的器件普遍具有耐高温特性，工作温度一般可以达到 300 ℃甚至以上[1]。为进一步发挥其优势并尽可能降低配套模块的制造成本，封装材料需要满足低温连接、高温服役的要求[2-4]。纳米银颗粒烧结技术作为一种满足该要求的互连方法，可使芯片与基板之间形成具有优良电学性能与导热性能的接头[5-9]。传统的纳米银烧结技术目前已经获得广泛研究并开始进入应用实验阶段，其基本原理是以化学方法制备纳米银颗粒并与有机组分混合，配制成纳米焊膏进行烧结连接[10-12]。但是，焊膏中普遍存在的有机组分也对连接层的烧结存在不利影响。例如，为了保证有机物在烧结过程中能够尽快分解且不使连接层发生开裂，必须在烧结保温过程之前追加预热或烘干工序，而对于具有复杂配方的焊膏而言，烧结工艺的复杂程度也随之增加；焊膏中的有机组分很难在低于 200 ℃的条件下分解，阻碍了银纳米颗粒在低温条件下的烧结过程。无有机物的纳米银贴片互连材料可避免上述问题，而使用超快激光作为光源的脉冲激光沉积（PLD）工艺是一种高效率制备大面积无有机物纳米银薄膜的有效方法[13-14]。以皮秒激光和飞秒激光为代表的超短脉冲激光具有极高的峰值功率，其作用于靶材时产生的离子动能高、易于通过气氛环境进行精细控制，从而可以制备具有独特结构的纳米薄膜[15-17]。该方法制备的纳米银薄膜中颗粒的尺寸分布多样且可以控制，其烧结温度可低至 180 ℃，无需进行预热、烘干，满足 SiC 功率器件对贴片互连材料的强度要求。

上述贴片互连材料的连接接头一般会在高温环境中服役，因此有必要验证其高温可靠性。高温存储（HTS）测试是检验接头耐受高温环境能力的常用测试方法，一般采用其剪切强度经过高保温后的变化情况作为评价指标[18]，主要关注连接层微观组织的演变对接头强度的影响[19]、长时间保温后接头的失效特点和机理[20]。目前，针对多孔烧结银接头开展的高温存储测试，一般使用焊膏作为原材料，多数在大气或真空环境下开展实验[21-24]。针对多孔连接层长时间保温的演变机制已有初步的共识：连接

收稿日期：2020-11-30；**修回日期**：2020-12-25；**录用日期**：2021-02-23

基金项目：国家重点研发计划(2017YFB1104900)、国家自然科学基金(51775299，52075287，51520105007)

* **E-mail**：zougsh@tsinghua.edu.cn

层内的多孔结构在保温过程中将呈现致密化到孔隙长大的演变过程，烧结接头的强度在长时间保温后明显下降[24]，该演变过程在真空环境中有受阻趋势[19]。然而，针对该孔隙演变现象的机理分析却存在一定的争议。目前已有多项研究表明氧化现象对纳米银材料的烧结过程存在影响[21,25-26]，且已有研究利用这一现象，使用氧化银微米颗粒烧结获得了多孔银连接层[27]。基于氧化现象，Lin 等[28]结合多晶银膜表面存在的火山喷发效应，认为大气环境下长时间保温过程中烧结银的多孔结构演变是氧化现象产生的小尺寸纳米银颗粒在烧结颈附近生成并再次烧结导致的。然而，Zhang 等[19]则认为焊膏烧结接头的组织演变过程不能简单归因于氧化现象（纳米银焊膏中常常包含一些分解难度较大的有机物[29-31]），大气环境可以使这些有机物在长时间保温中逐渐分解，而真空环境则会阻碍这一过程，进而影响到孔隙的演变进程；此外，真空条件下服役环境的气压也会发生变化，而连接层中很有可能存在烧结时形成的包含气体的封闭孔隙，这部分孔隙在真空条件下对连接层组织演变的影响仍需要深入研究。因此，有必要选择原始成分更为单一的多孔烧结银接头作为研究对象，进一步明确服役环境中影响连接层微观组织与性能的主导因素，为保障连接接头高温可靠性的优化工作提供更有针对性的依据和参考。使用脉冲激光沉积的复合纳米银膜制备烧结接头，即可获得不包含有机物的样本，对其开展气氛条件可变的高温存储实验，并与真空环境下的对照组进行比较，不仅可以有效推动前述争议的解决，也有利于进一步系统性地研究多孔烧结银组织在高温条件下的长期演变行为及其调控方法。

本文针对待连接母材，即 SiC 芯片和镀银陶瓷基板(DBC)，采用 PLD 技术，于氩气环境下仅在 SiC 芯片表面直接沉积不包含任何有机物的、由微米银颗粒和纳米银颗粒混合组成的银微纳颗粒复合薄膜，简称银复合薄膜(SMNCF)[14]。以该复合薄膜为中间层，在 180～300 ℃条件下进行 SiC 芯片与 DBC 的低温烧结连接。在此基础上，系统研究了烧结连接接头于不同气氛环境中经过 300 ℃条件下长时间保温存储后的室温剪切强度、烧结连接层微观组织的演变规律及其与保温气氛的关联性，深入探讨气氛中氧含量对接头连接层微观组织演变过程的影响规律。

2 实验方法

2.1 银微纳颗粒复合薄膜的 PLD 制备及微观表征

采用 PLD 方法和 99.99%纯度的银靶材，于氩气氛围下在待连接母材(SiC 芯片)表面沉积制备不含任何有机物的银微纳颗粒复合薄膜。沉积系统如图 1(a)所示，图 1(b)则是 SiC 芯片沉积前后的宏观

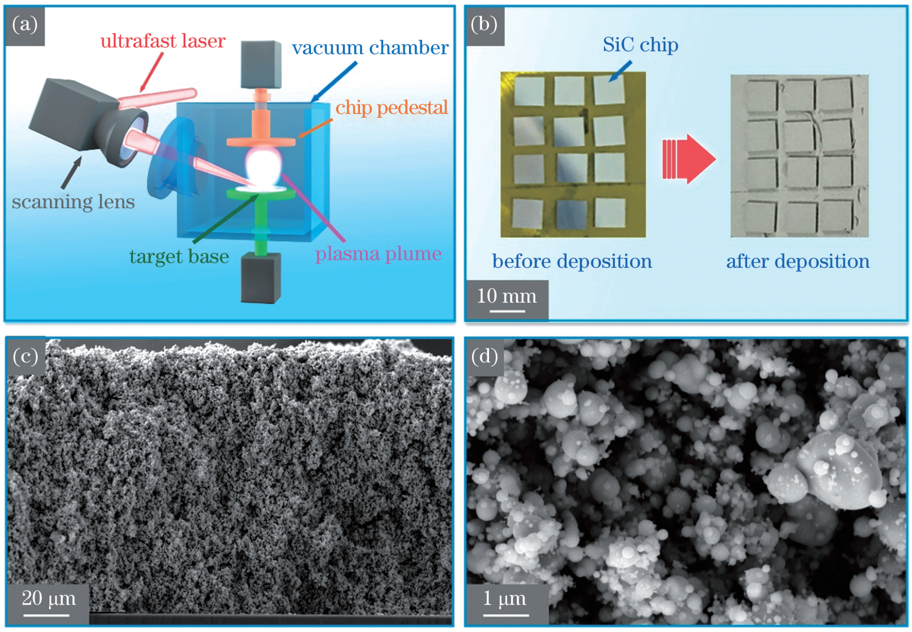

图 1 PLD 相关设备及实验过程。(a)PLD 设备与过程示意图；(b)沉积前后的 SiC 芯片；(c)沉积态银微纳颗粒复合薄膜的截面微观组织；(d)沉积态薄膜中的微米颗粒与纳米颗粒

Fig. 1 Devices and experiment process related with PLD. (a) Schematic of PLD device and process; (b) SiC chips before and after deposition; (c) cross section microstructure of deposited silver micro-and nano-particles composite film; (d) micro- and nano-particles in deposited film

形貌照片，可观察到沉积态薄膜为浅灰色。图 1(c)和(d)是沉积态薄膜的截面显微照片，可观察到薄膜由微米尺度和纳米尺度的银颗粒组成，厚度一般为 80～100 μm。表 1 为 PLD 方法的基本参数，根据前期的研究[14]，采用适当的氩气气压可控制复合薄膜的厚度、疏松度及膜内的微纳米颗粒尺寸分布。该薄膜在低温条件下可实现对 SiC 芯片与 DBC 之间的烧结连接且接头具有足够高的剪切强度。

表 1　PLD 过程的基本参数

Table 1　Basic parameters of PLD process

Pulse duration /ps	Pulse energy /μJ	Scanning speed /($\mathrm{m \cdot s^{-1}}$)	Argon pressure /Pa
12	152	1	500

2.2　银微纳颗粒复合薄膜的烧结连接及接头高温可靠性测试

将沉积有银微纳颗粒复合薄膜的 SiC 芯片贴装至镀银的 DBC 上组合成模组，如图 2(a)和(b)所示。之后采用自主研制的热压设备在 250 ℃温度、10 MPa 辅助压力条件下对模组烧结 30 min，图 2(c)为烧结完成后的芯片模组截面示意图。此外，使用包含多种粒径的银微纳颗粒复合焊膏[19]制备对照组样本并在大气条件下保温，与前述复合银薄膜的烧结接头进行比较。焊膏样本在烧结时先分别在 150 ℃、250 ℃条件下各自烘干 5 min，而后在 10 MPa 辅助压力下于 250 ℃保温 30 min，完成烧结过程。

连接接头样本的高温可靠性测试通过 HTS 实验进行，评价指标主要为连接层的剪切强度、截面孔隙率、平均孔隙截面面积。其中，HTS 实验分为两类：大气与真空环境下 2000 h 的长期实验(焊膏对照组的保温时间为 1500 h)、氧浓度可变氛围下 400 h 的短期实验。1)针对大气与真空环境对照组的长时间保温实验，使用小型箱式炉提供高温环境并放置样本，将另一部分样本封入石英管，抽真空封口作为对照组；2)针对可变氛围的 HTS 实验，图 2(d)所示的管式炉与混气装置提供相应测试气氛环境，通过调整通入石英管内的氧气与氩气的混合比例，实现常压条件下氛围可控的保温实验。在氧浓度可变氛围的 HTS 实验中，设置了 3 组氛围进行对照：其一，氩气常压环境下进行的惰性氛围对照组，用于确

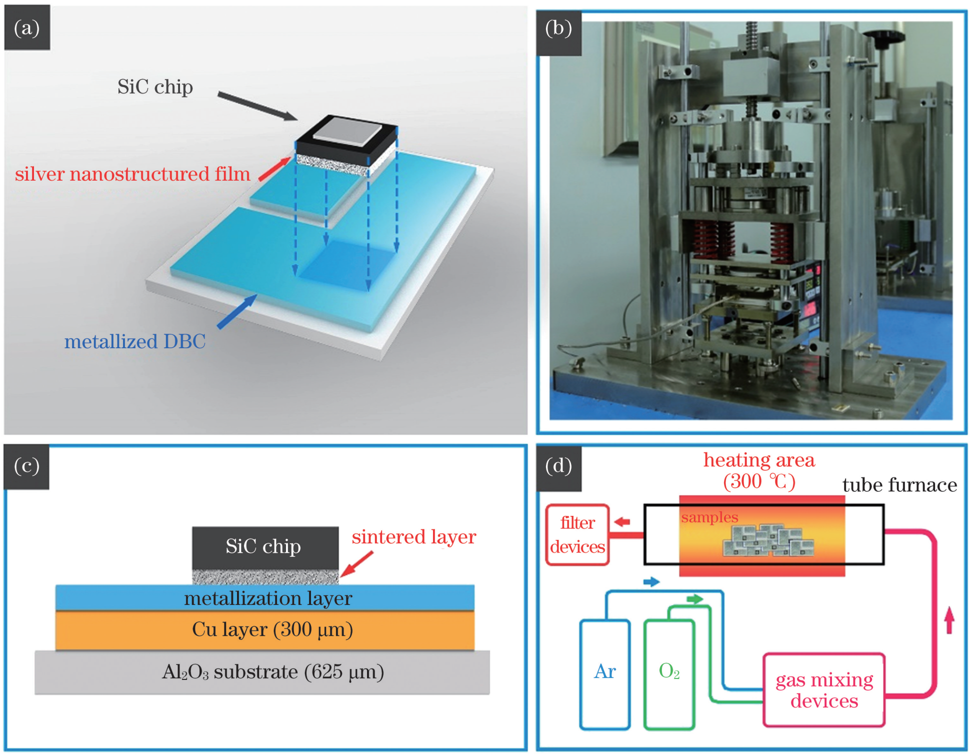

图 2　银微纳颗粒复合薄膜的烧结连接过程与可变气氛的 HTS 实验。(a)SiC 芯片的贴装；(b)自主研制的芯片模组辅助加压烧结互连设备实物图；(c)烧结完成的芯片模组截面示意图；(d)管式炉与混气装置的工作原理

Fig. 2　Sintering process using SMNCF and atmosphere-controllable HTS test. (a) Placement of SiC chip; (b) physical diagram of self-developed chip module auxiliary pressure sintering interconnection equipment; (c) schematic of the cross section of sintered sample; (d) working principle of tube furnace fixed with gas mixing device

认样本连接层的孔隙演变规律是否与真空环境下的一致，判断气压变化是否对连接层孔隙演变有影响；其二，氧浓度为 20% 的常压对照组，用于与大气环境下实验组进行对比，判断大气中的其他气体成分是否会对连接层孔隙演变有影响；其三，纯氧环境下的常压对照组，用于观察气氛全部为氧气时接头长时间保温过程中的连接层组织演变规律和纯氧对其演变的作用。

3 实验结果与讨论

3.1 大气与真空环境下高温存储实验中连接层的强度变化与组织演变过程

大气与真空环境中的高温存储接头样本形成对照，在检验银复合薄膜连接接头能否承受 300 ℃ 高温环境的同时，研究气氛对连接层力学性能和微观组织演变的影响。图 3 为 300 ℃ 保温 2000 h 过程中接头在室温下的剪切强度随保温时间的变化规律，图 4 为接头连接层微观组织演变规律，图 5 为其孔隙率、平均孔隙截面面积的统计结果。

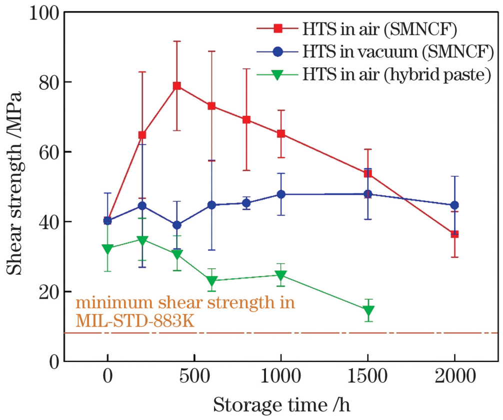

图 3 SMNCF 及复合银焊膏烧结连接接头的室温剪切强度随保温时间的变化情况

Fig. 3 Variation of shear strength of sintered joints using SMNCF and hybrid Ag paste on storage time

由图 3 可知，银复合薄膜低温烧结连接形成的多孔接头在 2000 h 保温过程中的剪切强度始终高于 20 MPa，明显高于美国军标MIL-STD-883K。使

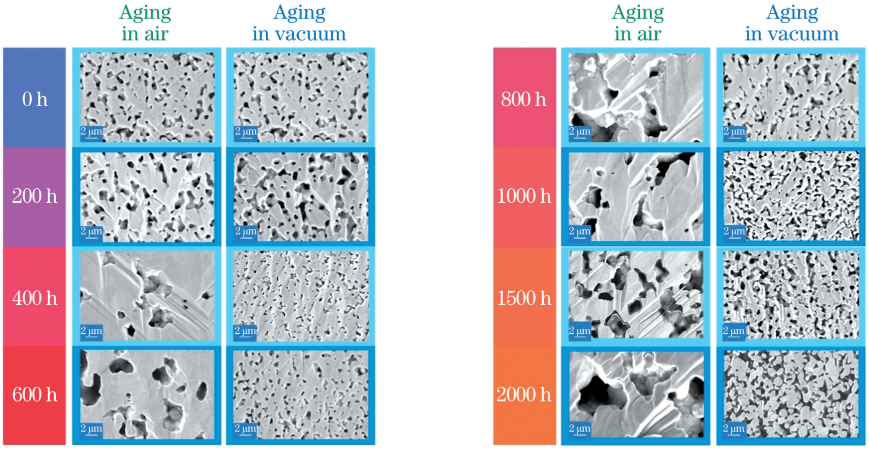

图 4 大气与真空环境下连接接头微观组织形貌随保温时间的变化

Fig. 4 Variation of microstructure of sintered joints with holding time under atmospheric and vacuum environments

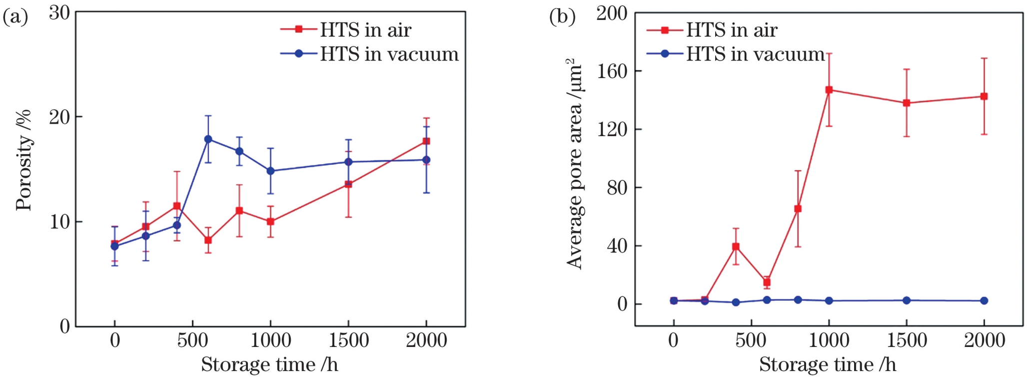

图 5 大气与真空环境下连接接头中的孔隙演变。(a) 孔隙率随保温时间的变化情况；(b)平均孔隙截面面积随保温时间的变化情况

Fig. 5 Pore evolutions in sintered joints under atmospheric and vacuum environments. (a) Variation of porosity with holding time; (b) variation of average pore cross section area with holding time

用复合焊膏的烧结连接层在长时间保温过程中的强度同样高于美国军标，但是明显低于银复合薄膜对照组，这可能是焊膏中包含了具有较高分解温度的有机组分所致。这部分有机物可有效防止焊膏在烧结过程中开裂，但是分解温度往往高于 300 ℃，因此其对连接层力学性能的影响有长期存在的可能。值得注意的是，大气与真空环境下复合银膜连接层的力学性能变化过程存在明显差异：大气环境保温的接头剪切强度在 0～400 h 保温期间呈现上升趋势，保温 400 h 时达到峰值（约 80 MPa），之后逐渐下降，并在保温至 2000 h 时降至最低（约 35 MPa），低于相同保温时间的真空对照组。而真空保温期间的接头强度变化不大，均值在 40～50 MPa 内波动，与烧结连接状态的接头没有明显区别。

上述差异与图 4 中的连接层截面微观组织演变存在一定关联性。由图 4 可见，大气环境下保温至 400 h 时连接层组织已经变得相对致密，而图 5(a)则表明其孔隙率相比初始状态呈现出上升趋势，这是由于孔隙平均截面面积增加了，如图 5(b)所示。相对于初始状态，该阶段连接层的孔隙率变化幅度仍在 3%以内，这表明孔隙在平均截面面积扩大的同时未能明显提升整个连接层的孔隙率。据此认为该阶段孔隙发生了聚集与合并，此时连接层内部将出现更多的致密区域。此结构的形成与银纳米颗粒烧结过程中连接颈的粗化过程类似，从而导致连接层内部强度的提升[32]。该现象也解释 400～1000 h 保温期间大气对照组接头样本的连接层孔隙率低于真空对照组，其剪切强度也更高的现象。

由图 5(b)可知，保温到 400～1000 h 时，大气对照组接头连接层最明显的变化是截面平均孔隙尺寸的扩大，其平均面积相对于初始状态增大了 20～25 倍，而在保温 1000～2000 h 间没有明显变化。与 0～400 h 保温过程不同的是，此类大尺寸孔隙的增加对连接层的弱化效应将会超过同时期生成的致密组织对连接层的强化效应，在使连接层孔隙率逐渐上升的同时，降低接头剪切强度，如图 5(a)所示。

综上，银复合薄膜低温烧结连接接头在长时间 300 ℃保温过程中的力学性能受到连接层多孔组织演变的影响。1）大气环境下：保温初期连接层孔隙存在合并的倾向与球化的趋势；在保温后期，孔隙的合并更为明显，且整体尺寸增大的同时形状也更不规则，连接层的整体孔隙率开始增加并最终影响到接头剪切强度。2）真空环境下：连接层孔隙的演变受到阻碍，因而接头的剪切强度相对于大气对照组接头更为稳定。

实验结果也表明，长时间在高温条件下，多孔连接层的组织演变过程与气氛环境存在密切的关联。本课题组对银纳米焊膏烧结连接接头的前期研究中同样存在类似的现象[19-20]，但是焊膏烧结后残留的有机组分使得该现象的机理分析难以继续深入：长时间保温后烧结组织中可能存在残留的有机物，其可能会阻碍连接层孔隙的演变，且难以被现有的分析手段检测到。真空环境可能在保温过程中阻碍了残留有机物的分解，因而在使用焊膏的材料体系中无法完全排除有机组分的影响。本实验采用了无有机物的烧结银接头，从源头上去除了有机组分对实验的干扰，因而可以确定气氛对烧结接头的组织演变过程存在重要影响。

然而，上述实验尚无法确认气氛对组织演变过程的影响究竟基于物理变化还是化学变化。对于物理变化，主要考虑气压差导致的孔隙演变：烧结后的连接层内普遍存在密闭孔隙，其中含有空气，将样本放置于真空环境中后此类孔隙内部的气体难以逸出，导致孔隙内外存在压力差。该压力差可能进一步导致孔隙尺寸及形貌在长期保温过程中发生变化。对于化学变化，主要考虑高温环境下银的氧化与氧化产物分解的动态过程导致的孔隙演变。本实验的保温高于所用银复合薄膜的烧结温度，同时也高于文献报道的纳米银颗粒氧化与产物分解动态过程发生的最低温度[28]，因而银的氧化与产物分解动态过程导致的原子迁移加速也有可能是孔隙演变的原因。因此，需要基于可变气氛的对照实验结果确认气氛影响多孔烧结组织演变的具体机理。

3.2 多孔烧结银连接层微观组织在氧浓度可变氛围下的高温存储实验

氧浓度可变氛围条件下的高温存储实验结果如图 6 所示。其中，采用孔隙率与平均孔隙截面面积作为评价指标描述连接层孔隙的变化过程，如图 6(g)和图 6(h)所示。结果表明：惰性常压氛围下的对照组的连接层孔隙演变趋势与真空条件下一致，孔隙率与平均孔隙截面面积相近，这表明气压对连接层长时间保温过程中的孔隙演变趋势不会产生明显影响；20%氧浓度对照组样本的连接层孔隙在保温至 400 h 时出现了与大气条件下类似的孔隙聚集与连接颈致密化趋势，表明大气中的其他气体对连接层孔隙演变产生的影响也不明显；100%氧浓度的常压对照组样本中，连接层的平均孔隙截面面积随保温时间增加显著扩大，且在保温 400 h后孔隙呈

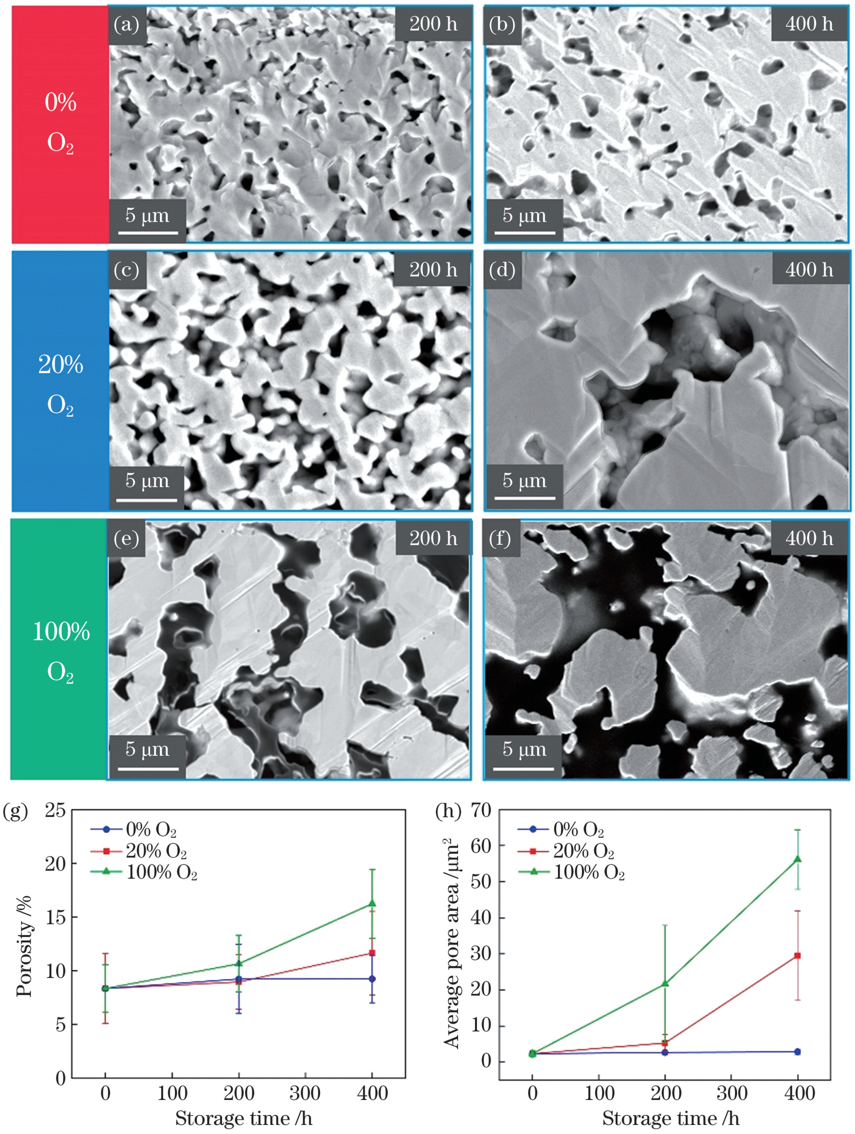

图 6 氧浓度可变的高温存储实验中连接层的微观组织演变。(a)(b) 惰性气体环境中保温 200 h 和 400 h 后连接层的微观组织;(c)(d) O_2 浓度 20%的气体环境中保温 200 h 和 400 h 后连接层的微观组织;(e)(f) O_2 浓度 100%的气体环境中保温 200 h 和 400 h 后连接层的微观组织;(g) 保温期间接头连接层孔隙率的变化规律;(h) 保温期间接头连接层平均孔隙截面面积的变化规律

Fig. 6 Microstructure evolutions of sintered layer during HTS tests in which the oxygen concentration is controllable. (a)(b) Microstructure of sintered layer in inert gas environment at heat preservation for 200 h and 400 h; (c)(d) microstructure of sintered layer in 20% concentration O_2 atmosphere at heat preservation for 200 h and 400 h; (e)(f) microstructure of sintered layer in 100% concentration O_2 atmosphere at heat preservation for 200 h and 400 h; (g) variation of porosity of sintered layer at heat preservation; (h) variation of average pore cross section area of sintered layer at heat preservation

现出连通趋势。在大气条件下,同样的趋势需要在保温时间超过 1000 h 后才能逐渐被观察到,且孔隙的连通现象没有纯氧条件下的明显。因此,长时间保温过程中烧结银组织的孔隙演变进程主要受到氧气与银的化学反应影响,大气环境是氧的主要来源。氧气作用于烧结组织时,其主要表现为孔隙截面面积扩大与连通的过程被加速。气压的变化基本不影响连接层孔隙的演变进程。

3.3 氧气对高温存储实验中连接层微观组织演变的影响分析

基于火山喷发效应[28],结合实验接头样本的显微观测结果,可以推测氧气对保温过程中孔隙演变进程的影响机制,如图 7 所示。由 PLD 方法制备的银复合薄膜中包含了大量有缺陷的微米颗粒与纳米

颗粒,这些缺陷在短时间的低温烧结过程中得以保留,形成图 7(a)、(b)所示的多晶结构。火山喷发效应指出,高温条件下氧气倾向于进入纳米银颗粒的晶界,从而形成一种液化的银氧化物,该氧化物在颗粒内部应力的作用下将向外挤出,如图 7(c)、(d)所示。由于环境温度高于氧化银纳米颗粒的分解温度,因而被挤出的银氧化物快速分解形成新的纳米银颗粒,而这部分颗粒在高于烧结温度的条件下将发生二次烧结,加速烧结过程中的原子迁移进程,如图 7(e)、(f)所示。真空或惰性气氛环境下的多孔烧结银组织中银原子的迁移主要依靠扩散过程,该过程在保温开始后较短的时间内便会因连接层内纳米结构的表面能逐步降低而难以继续进行,此时孔隙的演变将受到阻碍。而在具有一定氧浓度的氛围下,火山喷发效应的存在使得存储于连接层内缺陷中的能量以氧化物挤出的形式被释放,转换为新生成的小尺寸纳米颗粒的表面能,这使得银原子的迁移获得了额外的能量,烧结过程也得以继续推进。此外,由于挤出的银氧化物在高温条件下将再次分解,因而整个过程可以视作以氧气为催化剂的反应过程。降低保温气氛中的氧浓度,即可有效减缓连接层孔隙率变化而引发的接头力学性能、电学性能的变化,使封装结构在长时间保温过程中更为稳定、可靠。

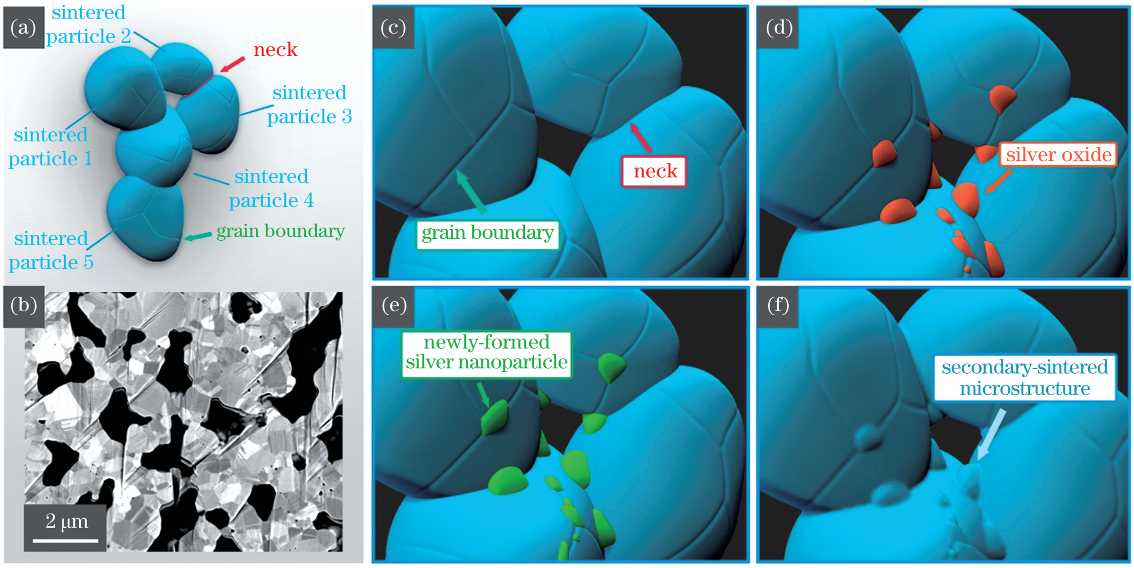

图 7 氧气对保温过程中接头连接层孔隙演变进程的影响机制。(a)经过烧结,包含连接颈与多个晶界的纳米颗粒团簇示意图;(b)保温前样本接头连接层中多晶结构的显微照片;(c)(d)火山喷发效应中银的氧化物在晶界与连接颈附近被挤出的示意图;(e)(f)挤出后的银氧化物动态分解形成新的纳米颗粒并发生二次烧结的过程示意图

Fig. 7 Influence mechanism of oxygen on pore evolution process of sintered joints during HTS tests. (a) Schematic of nanoparticle clusters with sintered necks and grain boundaries after sintering; (b) SEM image of polycrystalline structure in sintered layer before HTS tests; (c)(d) schematic of silver oxide extruded near grain boundaries and necks in nano-volcanic eruption effect; (e)(f) schematic of dynamic decomposition of extruded silver oxide and secondary sintering of newly-formed silver nanoparticles

4 结 论

采用 PLD 方法制备的无有机物银微纳颗粒复合薄膜低温烧结连接 SiC 芯片和镀银陶瓷基板,对烧结后的样本开展了不同气氛环境下的长时间保温实验。结果表明,烧结连接接头在 300 ℃条件保温 2000 h 期间的剪切强度始终高于 20 MPa,满足美国军标要求。连接层内的孔隙在高温存储过程中存在演变倾向,其总体趋势为孔隙的聚集与连通。该过程受到气氛中氧气的影响最明显,气压及大气环境中的其他气体成分对孔隙演变的影响较小。真空环境与惰性气氛环境中连接层组织在保温期间较为稳定,接头剪切强度波动不大,说明真空与惰性氛围均有利于提升多孔烧结银接头的高温可靠性。

致谢 本研究得到了清华大学机械工程系刘磊副教授的大力支持。

参 考 文 献

[1] Paknejad S A, Mannan S H. Review of silvernanoparticle based Die attach materials for high

power/temperature applications[J]. Microelectronics Reliability, 2017, 70: 1-11.

[2] Mei Y H, Feng J J, Wang X M, et al. Medium and high voltage IGBT module using nanosilver paste sintering technology and its performance characterization [J]. High Voltage Engineering, 2017, 43(10): 3307-3312.
梅云辉, 冯晶晶, 王晓敏, 等. 采用纳米银焊膏烧结互连技术的中高压 IGBT 模块及其性能表征[J]. 高电压技术, 2017, 43(10): 3307-3312.

[3] Xiao Y. Study on low temperature sintering mechanism and performance of composite silver nanoparticles [D]. Harbin: Harbin Institute of Technology, 2016: 30-35.
肖勇. 复合纳米银颗粒低温烧结机理及其性能研究[D]. 哈尔滨: 哈尔滨工业大学, 2016: 30-35.

[4] Chen G, Wang Y Z, Mei Y H, et al. Influence of sintering process on microstructure of nanosilver paste[J]. Heat Treatment of Metals, 2016, 41(5): 103-108.
陈刚, 王一哲, 梅云辉, 等. 烧结工艺对纳米银焊膏微观结构的影响[J]. 金属热处理, 2016, 41(5): 103-108.

[5] Li M Y, Xiao Y, Zhang Z H, et al. Bimodalsintered silver nanoparticle paste with ultrahigh thermal conductivity and shear strength for high temperature thermal interface material applications [J]. ACS Applied Materials & Interfaces, 2015, 7(17): 9157-9168.

[6] Blank T, Ishikawa D, An B N, et al. Low temperature silver sinter processes on (EN) EPEAg surfaces for high temperature SiC power modules[C]//10th International Conference on Integrated Power Electronics Systems, March 20-22, 2018, Stuttgary, Germany. New York: IEEE Power Electronics Society, 2018.

[7] Guo W, Zeng Z, Zhang X Y, et al. Low-Temperature sintering bonding using silver nanoparticle paste for electronics packaging [J]. Journal of Nanomaterials, 2015: 10.

[8] Feisst M, Schaetzle P, Wilde J. Power chip interconnections based on TLP and sintering of CTEMatched conductors [C] // 10th International Conference on Integrated Power Electronics Systems, March 20-22, 2018, Stuttgary, Germany. New York: IEEE Power Electronics Society, 2018.

[9] Chew L M, Schmitt W, Nachreiner J, et al. Silver sinter paste optimized for pressure sintering under air atmosphere on precious and non-precious metal surfaces with high reliable sintered [C] // 10th International Conference on Integrated Power Electronics Systems, March 20-22, 2018, Stuttgary, Germany. New York: IEEE Power Electronics Society, 2018.

[10] Rodríguez-Sánchez L, Blanco M C, López-Quintela M A. Electrochemical synthesis of silver nanoparticles[J]. The Journal of Physical Chemistry B, 2000, 104(41): 9683-9688.

[11] Huang H H, Ni X P, Loy G L, et al. Photochemical formation of silver nanoparticles in poly (N-vinylpyrrolidone)[J]. Langmuir, 1996, 12(4): 909-912.

[12] Sun Y, Xia Y. Shape-controlled synthesis of gold and silver nanoparticles[J]. Science, 2002, 298(5601): 2176-2179.

[13] Feng B, Shen D Z, Wang W G, et al. Cooperative bilayer of lattice-disordered nanoparticles as room-temperature sinterable nanoarchitecture for device integrations [J]. ACS Applied Materials & Interfaces, 2019, 11(18): 16972-16980.

[14] Wang W G, Zou G S, Jia Q, et al. Mechanical properties and microstructure of low temperature sintered joints using organic-free silver nanostructured film for Die attachment of SiC power electronics[J]. Materials Science and Engineering: A, 2020, 793: 139894.

[15] Cheng Y, Lu Y M, Guo Y L, et al. Development of function films prepared by pulsed laser deposition technology[J]. Laser & Optoelectronics Progress, 2015, 52(12): 120003.
程勇, 陆益敏, 郭延龙, 等. 脉冲激光沉积功能薄膜的研究进展[J]. 激光与光电子学进展, 2015, 52(12): 120003.

[16] Fan L S, Zhang S W, Zhang Q L, et al. Research progress on fabrication of one-dimensional well-ordered oxide nanostructures by pulsed laser deposition[J]. Laser & Optoelectronics Progress, 2020, 57(19): 190001.
范丽莎, 张硕文, 张群莉, 等. 脉冲激光沉积制备一维有序氧化物纳米结构的研究进展[J]. 激光与光电子学进展, 2020, 57(19): 190001.

[17] Mo G K, Liu J H, Zou Z L, et al. Preparation of low-resistivity GZO thin films using pulsed laser deposition and investigation of optoelectronic properties[J]. Chinese Journal of Lasers, 2019, 46(10): 1003001.
莫观孔, 刘家辉, 邹卓良, 等. 脉冲激光沉积法制备低阻掺镓氧化锌薄膜及其光电性能[J]. 中国激光, 2019, 46(10): 1003001.

[18] Paknejad S A, Dumas G, West G, et al. Microstructure evolution during 300 ℃ storage of sintered Ag nanoparticles on Ag and Au substrates

[J]. Journal of Alloys and Compounds, 2014, 617: 994-1001.

[19] Zhang H Q, Wang W G, Bai H L, et al. Microstructural and mechanical evolution of silver sintering Die attach for SiC power devices during high temperature applications[J]. Journal of Alloys and Compounds, 2019, 774: 487-494.

[20] Zhang H Q, Zhao Z Y, Zou G S, et al. Failure analysis and reliability evaluation of silver-sintered Die attachment for high-temperature applications[J]. Microelectronics Reliability, 2019, 94: 46-55.

[21] Chen C T, Choe C, Kim D, et al. Effect of oxygen on microstructural coarsening behaviors and mechanical properties of Ag sinter paste during high-temperature storage from macro to micro[J]. Journal of Alloys and Compounds, 2020, 834: 155173.

[22] Egelkraut S, Frey L, Knoerr M, et al. Evolution of shear strength and microstructure of Die bonding technologies for high temperature applications during thermal aging[C]//2010 12th Electronics Packaging Technology Conference, December 8-10, 2010, Singapore. New York: IEEE Press, 2010: 660-667.

[23] Lang F Q, Nakagawa H, Aoyagi M, et al. Impact of joint materials on the reliability of double-side packaged SiC power devices during high temperature aging[J]. Journal of Materials Science: Materials in Electronics, 2010, 21(9): 917-925.

[24] Yu F, Cui J Z, Zhou Z M, et al. Reliability of Ag sintering for power semiconductor Die attach in high-temperature applications[J]. IEEE Transactions on Power Electronics, 2017, 32(9): 7083-7095.

[25] Zhang Z, Chen C T, Yang Y, et al. Low-temperature and pressureless sinter joining of Cu with micron/submicron Ag particle paste in air[J]. Journal of Alloys and Compounds, 2019, 780: 435-442.

[26] Chen C T, Suganuma K. Microstructure and mechanical properties of sintered Ag particles with flake and spherical shape from nano to micro size[J]. Materials & Design, 2019, 162: 311-321.

[27] Mu F W, Zou G S, Zhao Z Y, et al. Low temperature sintering-bonding through *in situ* formation of Ag nanoparticles using micro-scaled Ag_2O composite paste[J]. Transactions of the China Welding Institution, 2013, 34(4): 38-42, 115.
母凤文, 邹贵生, 赵振宇, 等. 微米氧化银膏原位生成纳米银的低温烧结连接[J]. 焊接学报, 2013, 34(4): 38-42, 115.

[28] Lin S K, Nagao S, Yokoi E, et al. Nano-volcaniceruption of silver[J]. Scientific Reports, 2016, 6: 34769.

[29] Bu L, Ching W L, Ling H S, et al. 3-D modeling and characterization for Die attach process[J]. IEEE Transactions on Components, Packaging and Manufacturing Technology, 2016, 6(10): 1567-1575.

[30] Zhang H Q, Zou G S, Liu L, et al. Low temperature sintering of silver nanoparticle paste for electronic packaging[C]//2016 International Conference on Electronics Packaging (ICEP), April 20-22, 2016, Hokkaido, Japan. New York: IEEE Press, 2016: 314-317.

[31] Schmitt W, Chew L M, Miller R. Pressureless sintering of large dies by infrared radiation[C]//10th International Conference on Integrated Power Electronics Systems, March 20-22, 2018, Stuttgary, Germany. New York: IEEE Power Electronics Society, 2018.

[32] Yu F, Cui J Z, Zhou Z M, et al. Reliability of Ag sintering for power semiconductor Die attach in high-temperature applications[J]. IEEE Transactions on Power Electronics, 2017, 32(9): 7083-7095.

Microstructureand Property Evolutions of Joints Sintered by Silver Micro- and Nano-particles Composite Film

Wang Wengan, Jia Qiang, A Zhanwen, Feng Bin, Zhao Wenzheng, Bai Hailin, Zou Guisheng*

State Key Laboratory of Tribology, Department of Mechanical Engineering, Tsinghua University,
Beijing 100084, *China*

Abstract

Objective With the application of new generation power electronic devices, their advantages in severe working conditions are gradually emerging. For instance, SiC power devices can serve in high-temperature conditions over 300 ℃, and their packaging materials should be bonded at low temperature (≤250 ℃) and work reliably in high-temperature conditions. Sintering silver nanoparticles (NPs) technology is an effective method that can form joints with excellent electrical and thermal properties between SiC chips and metallized substrates. The traditional silver NP-sintering technology is synthesizing NPs by a chemical method and mixing them with organic components to prepare pastes. However, the adverse effects of organic components in the pastes can reduce the performance of sintered joints; thus, organic-free solutions have emerged recently. Pulsed laser deposition (PLD) with ultrafast laser as the light source is an efficient method to prepare organic-free silver-nanostructured films with large areas. Ultrafast laser with a very high peak power can ablate a target and produce ions with high kinetic energy, which can be controlled by the atmosphere to form films with unique nanostructures. In this study, organic-free silver micro-particle and NP composite film (SMNCF) was prepared by a PLD method on SiC chips. The films were used as intermediate layers for the low-temperature sintering process to bond SiC chips and metallized ceramic substrates. The size distribution of the as-prepared nanosilver films is diverse and controllable, and the sintering temperature can be as low as 180 ℃, which meets the shear strength requirements of SiC power devices.

Methods In this study, SiC chips with deposited SMNCF were mounted on silver metallized substrates to form modules. These modules were sintered at 250 ℃ with 10 MPa applied pressure for 30 min. In addition, samples in control groups were prepared with hybrid silver NP pastes. The modules were dried at 150 ℃ for 5 min and then maintained at 250 ℃ for 30 min under 10 MPa applied pressure to complete the sintering process. High-temperature storage (HTS) is a general method to verify the reliability of sintered layers using SMNCF, and it mainly focuses on the change of shear strength after tests and the influence of microstructure evolution in sintered layer. The HTS tests were performed at 300 ℃, and cross-sectional samples of sintered joints after tests were prepared to observe the microstructure of the sintered layer. Shear strength, porosity, and average pore area of sintered layer were measured. In addition, the HTS tests were divided into two categories: long-term tests in the atmospheric and vacuum environments for 2000 h (holding time of the control group using hybrid paste is 1500 h) and short-term tests at varying oxygen concentrations for 400 h. In the HTS test with varying atmosphere, three groups of the atmosphere were set for comparison: inert atmosphere using argon, which was used to confirm whether the pore evolution in the sintered layer was consistent with the samples in the vacuum environment; atmosphere with 20% oxygen concentration, which was used for comparison with the atmospheric environment; and a pure oxygen environment, which was used to observe the effect of pure oxygen on the microstructure evolution of sintered layer.

Results and Discussions Test results (Fig. 3–5) show that the shear strength of sintered joints was always higher than 20 MPa in the HTS test at 300 ℃ for 2000 h, which was significantly higher than the standard MIL-STD-883K. Besides, although the shear strength of sintered joints using hybrid NP paste is also higher than the standard MIL-STD-883K, it is significantly lower than the control groups using SMNCF. This is attributable to the residual organic components in sintered layer with decomposition temperature higher than 300 ℃, which would affect the mechanical properties of sintered joints. During 0–400 h in the atmospheric environment, the pores in sintered layer gradually accumulated and led to densification of sintered layer, which increased the shear strength of the joints; during 400–2000 h, the accumulation of pores led to a continuous expansion of the pores, which increased the porosity and decreased the shear strength of joints. The vacuum environment hindered the evolution of pores in sintered layer (Fig. 6). The increase in oxygen concentration in the atmosphere can accelerate the evolution process of the sintered layer during HTS tests. The influence of oxygen concentration on the mechanism of the microstructure evolution was discussed (Fig. 7).

Conclusions In this study, organic-free SMNCF was fabricated by the PLD method and a low-temperature sintering process was performed to obtain porous joints between SiC chips and silver metallized substrates. HTS tests were performed in different atmospheres. The results show that the shear strength of the sintered joints is always higher than 20 MPa at 300 ℃ for 2000 h. The pore aggregation and connectivity during the tests can be observed in the atmosphere, and this phenomenon is mostly influenced by the oxygen concentration in the atmosphere, while the ambient pressure and other gas components in the atmosphere have an insignificant influence on the pore evolution. In vacuum and inert atmosphere, the microstructure of the sintered layer is relatively stable in the HTS tests, and there was no significant change in shear strength of the joints. This indicates that both vacuum and inert atmosphere are beneficial to improve the high-temperature reliability of the porous sintered joints using SMNCF.

Key words laser technique; materials; silver micro- and nano-particles composite film; pulsed laser deposition; low temperature sintering joining; high temperature reliability

OCIS codes 160.4236; 140.3470; 310.6845